



Effect of Synthesized Conditions of Cu-K-OMS-2 on Toluene Oxidation Performance

Chatkamol Kaewbuddee^{1,2}, Narong Chanlek³, Kitirote Wantala^{1,2,4,5,*}

¹ Department of Chemical Engineering, Faculty of Engineering, Khon Kaen University, Khon Kaen 40002, Thailand

² Chemical Kinetics and Applied Catalysis Laboratory (CKCL), Faculty of Engineering, Khon Kaen University, Khon Kaen 40002, Thailand

³ Synchrotron Light Research Institute (Public Organization), 111 University Avenue, Muang District, Nakhon Ratchasima, 30000, Thailand

⁴ Research Center for Environmental and Hazardous Substance Management (EHSM), Faculty of Engineering, Khon Kaen University, Khon Kaen 40002, Thailand

⁵ Center of Excellence on Hazardous Substance Management (HSM), Chulalongkorn University, Bangkok 10330, Thailand

* Corresponding author: Email: kitirote@kku.ac.th

Article History

Submitted: 18 September 2019/ Revision received: 18 October 2019/ Accepted: 25 October 2019/ Published online: 3 December 2019

Abstract

The objective of this study was to optimize synthesis conditions for the Cu-K-OMS-2 hydrothermal process. The effects of ageing temperature, ageing time and amount of copper (Cu) dopant were considered via using the Box-Behnken design (BBD) method to characterize the conditions for gaseous toluene degradation. In the models studied, the independent variables were ageing temperature (55-145°C), ageing time (6-18 h) and amount of Cu dopant (2-6% mole). The quadratic model fitted very well with the experimental data (15 runs), which showed a higher value of R^2 (0.98) and adjusted R^2 (0.95), confirming that the model can explain the results successfully. Ageing temperature was found to be the only significant variable for the Cu-K-OMS-2 transformation phase, with CuO and the bixbyite phase appearing as the highest ageing temperature condition. Furthermore, the effects of ageing temperature, ageing time and amount of Cu dopant on the $\text{Cu}^{3+}/\text{Cu}^{2+}$ mole ratio were also investigated. Ageing temperature and amount of Cu dopant displayed a significant effect on both toluene removal and the $\text{Cu}^{3+}/\text{Cu}^{2+}$ mole ratio. On the other hand, ageing time was not significant for both responses. The high $\text{Cu}^{3+}/\text{Cu}^{2+}$ mole ratio led to enhancement of toluene removal. The optimized conditions for Cu-K-OMS-2 synthesis were determined as 120°C of ageing temperature, 6 h of ageing time and 6% by mole of Cu on K-OMS-2, which removed 80% of toluene at a reaction temperature of 180°C.

Keywords: $\text{Cu}^{3+}/\text{Cu}^{2+}$ ratios; VOC oxidation; Cryptomelane; Hydrothermal conditions; XPS

Introduction

Toluene is a volatile organic compound (VOC) and a significant environmental contaminant. Exposure can cause acute and chronic effects in the human body, including headache, nausea, sleepiness, cardiac arrhythmia, cancer and damage to the central nervous system [1-4]. Toluene is widely used as a raw material in production of organic compounds and as a solvent in many household products. In addition, it is added to gasoline to improve octane ratings. Elevated concentrations of toluene can result in indoor air from common household products and in outdoor air from transportation. There is growing concern at global level over VOC contamination in the environment [5]. Numerous technologies for removal of gaseous toluene are available, including incineration, catalytic incineration, adsorption and condensation processes, photocatalysis, biodegradation, catalytic combustion and thermal catalytic oxidation [6-10]. Among these techniques, thermal catalytic oxidation is accepted as an efficient, economically feasible and environmentally friendly method, based on oxidation of toluene into carbon dioxide and water [11-14].

Copper (Cu)-modified cryptomelane has been widely used for the improvement of the performance of cryptomelane-type octahedral molecular sieves (K-OMS-2) in VOC degradation [15-18]. Yun et al. [19] synthesized a Cu/OMS-2 nanocomposite with different Cu/manganese (Mn) molar ratios using an impregnation method. Catalytic activity was tested by reduction of NO in a continuous flow fixed-bed quartz tubular reactor. The results showed that the CuO/OMS-2 samples significantly improved NO conversion and N₂ yield, compared with pure OMS-2 and nano CuO. Moreover, the CuO in the CuO/OMS-2 samples existed in the monoclinic CuO phase. Nano CuO is predominant at increased Cu/Mn molar ratio. Furthermore, the Cu was doped in OMS-2 by

solid-state reaction. The OMS-Cu material displayed very high catalytic activity for total oxidation of CO in comparison to the OMS-2. The high activity of OMS-Cu material was associated with high lattice oxygen mobility and availability due to formation of Cu-Mn-O bridges. The interaction of Cu-Mn in the lattice oxide was due to charge delocalization effects and generation of active sites for CO oxidation reaction [20]. Likewise, Sun et al. [21] prepared transition metals doped with OMS-2 catalyst under reflux conditions. They proposed that Cu²⁺ doped OMS-2 catalyst can improve combustion of dimethyl ether at low reaction temperature because of the richer defect-oxide species. Additionally, the formation of Cu-O-Mn bridge in Cu-OMS-2 catalyst led to high reducibility, resulting in high mobility of oxygen species. Moreover, the Cu-OMS-2 catalyst could be re-oxidized to its original state after reduction. Therefore, after one reduction-reoxidation cycle, the Cu-OMS-2 became easier to reduce. According to reviews, the presence of Cu in K-OMS-2 catalyst can improve the physicochemical properties and its performance. Preparation methods can affect the formation of catalyst and resulting catalytic activity. Cu-doped K-OMS-2 catalyst showed high activity compared with un-doped K-OMS-2 catalyst because it presented excellent properties such as phase structure, lattice oxygen mobility, defect-oxide species and reducibility.

Normally, active catalysts depend on hydrothermal synthesis conditions including ageing temperature, ageing time, concentration of precursors and pH of solutions [22-27]. In order to study these multivariate effects, response surface methodology (RSM) was used as a tool for optimization of the preparation parameters [28]. RSM consists of mathematical and statistical techniques based on the fit of models to empirical experimental data. The RSM is used for improving and optimizing the processes. The Box-Behnken experimental

design (BBD) is widely used with RSM to fit a model using the least squares technique, and to optimize chemical and physical processes [28-32]. Yodsa-nga et al. [33] studied the effect of hydrothermal conditions for K-OMS-2 synthesis following RSM using central composite design (CCD) method. They found that formation of K-OMS-2 crystalline structure depended on both ageing temperature and time. The K-OMS-2 transformed to K-OMS-7 when K-OMS-2 was synthesized at high ageing temperature and time. The higher ageing temperature resulting in low specific surface area and Mn^{3+}/Mn^{4+} ratios of K-OMS-2 catalyst. Moreover, the K-OMS-2 sample at an ageing temperature of 75°C and 21 h of ageing time was found to be optimal as a catalyst for benzene removal. Likewise, Millanar et al. [34] confirmed that the hydrothermal temperature and time have significant effects on toluene removal using the K-OMS-2 catalyst. Toluene removal decreased with increasing ageing temperature. While removal efficiency increased when ageing temperature was increased from 75°C to 120°C, further increase from 120°C to 165°C caused a significant decrease in catalytic performance. Therefore, the hydrothermal synthesis conditions affect physicochemical properties including structure, active phase, specific surface area, morphology and crystallinity of the catalyst, which affected the catalytic performance.

Recently, we were able to dope a high-valent Cu into the K-OMS-2 framework structure (Cu-K-OMS-2) using the *in situ* hydrothermal method. Therefore, the aim of this work was to synthesize cryptomelane catalyst by doping with Cu via the *in situ* hydrothermal technique. Physical property such as crystalline phase of catalyst was analyzed by X-ray diffractometer (XRD). Moreover, oxidation of Cu species in K-OMS-2 framework structure were confirmed by X-ray photoelectron spectroscopy (XPS). In order to study the effect

of preparation parameters on Cu-K-OMS-2 synthesis, the ageing temperature, ageing time and amount of Cu dopant on Cu-K-OMS-2 catalyst were designed by BBD. The influence of synthesis variables on main and interactive effects were explained by using toluene oxidation and Cu^{3+}/Cu^{2+} mole ratio as responses. Moreover, the optimal conditions for Cu-K-OMS-2 synthesis were estimated.

Materials and methods

1) Chemicals and Cu-K-OMS-2 synthesis

Manganese (II) acetate tetrahydrate ($Mn(CH_3COO)_2 \cdot 4H_2O$, 99%), potassium permanganate ($KMnO_4$, 99%), glacial acetic acid (CH_3COOH) and Cu AAS standard solution (1000 ppm) were used as precursors for Cu-K-OMS-2 synthesis, and were purchased from ACROS Organics, UNIVAR, QRëC and Applichem, respectively. The Cu-K-OMS-2 catalysts were synthesized by a hydrothermal method, following previous work [33]. First of all, the $KMnO_4$ and $(Mn(CH_3COO)_2)$ solutions were prepared separately with deionized water under continuous stirring for 4 h. Then, the $KMnO_4$ solution was dropped into the $(Mn(CH_3COO)_2)$ solution. After that, proportional volumes for 2%, 4% and 6% moles of Cu standard solution were added into the mixture under continuous stirring. Then, the mixed solution was adjusted pH to an acidic condition via using concentrated glacial acetic acid. The final solution was transferred into an autoclave for hydrothermal process in various conditions (15 conditions) according to the BBD method with 3 factors and 3 levels (Table 1). Lastly, the obtained black slurry was washed with deionized water and dried overnight at 100°C to obtain the black Cu-K-OMS-2 samples.

2) Catalyst characterizations

The catalyst phase of all samples was analyzed by XRD (PANalytical, EMPYREAN, Netherlands) using Cu $K\alpha$ with wavelength

($\lambda=0.1514$ nm) at 40 mA and 45 kV. The oxidation states of Cu were determined by XPS techniques (BL5.3), Synchrotron Light Research Institute (Public Organization), Thailand.

3) Catalytic activity test with toluene oxidation

The catalytic activities of all Cu-K-OMS-2 samples were tested using gaseous toluene oxidation through a packed bed reactor (PBR). The Cu-K-OMS-2 samples (0.01 g) were packed in the center of the PBR. To control gas evaporation, the toluene solution was placed in a cold bath at -3°C . The toluene concentration (7,550 ppmV) was calculated following Doucet et al. [35]. For all experiments, the toluene

oxidation was examined with the weight hourly space velocity (WHSV) at 3.41 h^{-1} and the reaction temperature was studied in the range of $160\text{-}300^{\circ}\text{C}$. The quantity of toluene was measured by gas chromatography with thermal conductivity detector using Gaskuropack 54 as a column (GC-TCD, Shimadzu, 8A series, Japan), which repeatedly tested at least 3 times for each experiment. The percentage removal of toluene (Y_{exp}) was calculated by Eq 1.

$$Y_{\text{exp}} = \frac{C_0 - C_f}{C_0} \times 100\% \quad (\text{Eq. 1})$$

where C_0 and C_f are the initial and final toluene concentrations, respectively.

Table 1 Factors and level factors for design experiment by BBD

Variables	Factors			
	X	Low (-1)	Medium (0)	High (+1)
Ageing temperatures, ($^{\circ}\text{C}$)	X_1	55	100	145
Ageing time, (h)	X_2	6	12	18
Amount of Cu dopant, (%mole)	X_3	2	4	6

Results and discussion

1) Results of statistical analysis

The BBD method was used to study the effect of synthesis variables on gaseous toluene degradation and to determine the optimal condition for Cu-K-OMS-2 synthesis. The significant variables, including ageing temperature (X_1), ageing time (X_2) and amount of Cu dopant (X_3) with three levels, investigated designed using BBD. A total of 15 synthesis conditions were evaluated, and are summarized in Table 2. The activity of Cu-K-OMS-2 catalysts were tested by toluene oxidation and Y_{exp} was calculated following

Eq. 1 and used as a response. In addition, the oxidation states of Cu were analyzed by the XPS technique, which presented the Cu^{3+} and Cu^{2+} species (Figure 1) [36-39]. The $\text{Cu}^{3+}/\text{Cu}^{2+}$ mole ratio of each sample was computed, based on the fitting results of the XPS spectra, which was used for another response. The result of the 15 experiments together with both observed responses are summarized in Table 2. The regression coefficients were calculated by using Least-square of error as shown in Table 3. Accordingly, the predicted values of toluene removal and $\text{Cu}^{3+}/\text{Cu}^{2+}$ mole ratio based on the experimental and XPS results were evaluated using Eq. 2 and Eq. 3, respectively.

$$Y_1 (\%) = 63.603 + 18.415X_1 - 3.484X_2 + 3.149X_3 - 37.335X_1^2 + 4.472X_2^2 + 3.112X_3^2 - 4.020X_1X_2 + 6.595X_1X_3 + 0.208X_2X_3 \quad (\text{Eq. 2})$$

$$Y_2 = 2.600 - 0.223X_1 + 0.067X_2 + 0.128X_3 - 0.522X_1^2 - 0.188X_2^2 - 0.007X_3^2 - 0.301X_1X_2 + 0.054X_1X_3 + 0.034X_2X_3 \quad (\text{Eq. 3})$$

where Y_1 and Y_2 are predicted the percentage removal of toluene at 180°C of reaction temperature and $\text{Cu}^{3+}/\text{Cu}^{2+}$ mole ratio, respectively. X_1 , X_2 and X_3 were corresponding coded variables of ageing temperature, ageing time and amount of Cu dopant, respectively. X_1^2 , X_2^2 and X_3^2 were the square terms of coded independent variables and X_1X_2 , X_1X_3 and X_2X_3 were interaction terms of coded independent variables.

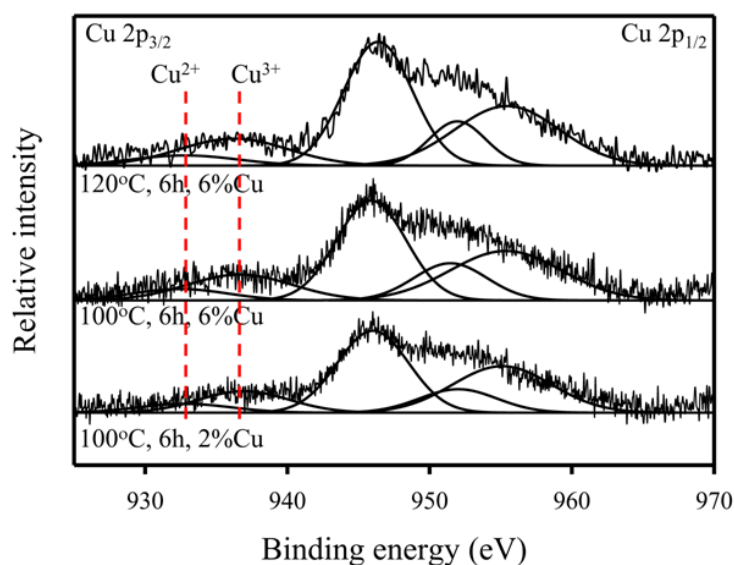


Figure 1 The XPS spectra of Cu-K-OMS-2 samples

Table 2 The Box-Behnken design of three variables together with both observed respond

Run order	Variables			Responses	
	X_1 (°C)	X_2 (h)	X_3 (%mole)	Y_{exp} (%)	$\text{Cu}^{3+}/\text{Cu}^{2+}$ mole ratio
1	145	6	4	55.40	1.76
2	145	12	2	34.89	1.69
3	55	12	2	12.76	2.16
4	55	18	4	14.12	2.62
5	145	18	4	44.42	1.49
6	100	12	4	66.46	2.60
7	100	18	2	64.74	2.23
8	100	6	6	77.22	2.52
9	100	18	6	66.64	2.52
10	100	12	4	66.91	2.55
11	55	6	4	9.02	1.69
12	100	12	4	57.44	2.64
13	55	12	6	10.68	2.34
14	100	6	2	76.15	2.36
15	145	12	6	59.19	2.09

Note: Y_{exp} values were measured at 180°C of reaction temperature.

Table 3 Estimated regression coefficients of toluene removal and $\text{Cu}^{3+}/\text{Cu}^{2+}$ mole ratio

Variables	Toluene removal (%)		$\text{Cu}^{3+}/\text{Cu}^{2+}$ mole ratio	
	Coefficients	P-value	Coefficients	P-value
Constant	63.603		2.600	
Ageing temperature	18.415	0.000	-0.223	0.006
Ageing time	-3.484	0.122	0.067	0.239
Amount of Cu dopant	3.149	0.154	0.128	0.049
Ageing temperature*Ageing temperature	-37.335	0.000	-0.522	0.001
Ageing time*Ageing time	4.472	0.166	-0.188	0.050
Amount of Cu dopant*Amount of Cu dopant	3.112	0.310	-0.007	0.922
Ageing temperature*Ageing time	-4.020	0.190	-0.301	0.008
Ageing temperature*Amount of Cu dopant	6.595	0.055	0.054	0.476
Ageing time*Amount of Cu dopant	0.208	0.941	0.034	0.653

Figure 2 displays the probability plot for the standardized residual for regression with the toluene removal data and $\text{Cu}^{3+}/\text{Cu}^{2+}$ mole ratio to determine the distribution assumption of the data. The significance of the regression equation at 95% confidence interval, the probability plot showed that the plotted points of both responses followed the fitted line, indicating that the assumptions were appropriate. Moreover, the predicted toluene removal and actual observed values were compared using the correlation values coefficient, in which R^2 and R^2_{adj} are 0.98 and 0.95, respectively. Close correspondence between R^2 and R^2_{adj} indicated a satisfactory approximation between the predicted model and actual observed values of toluene degradation efficiency. The predicted models were examined by the time series plot of fitted values (FITS) and actual observed values of toluene removal (Y_{exp}) and $\text{Cu}^{3+}/\text{Cu}^{2+}$ mole ratio, as shown in Figure 3(a) and (b), respectively. On this plot, the fitted values of both responses closely follow the actual observed data, which indicated that the predicted models fitted the experimental data. We can conclude that the errors of all run orders are insignificant. According to ANOVA results, F_{values} of the Lack of Fits (LoF) for both toluene removal and $\text{Cu}^{3+}/\text{Cu}^{2+}$ mole ratio were about 0.97 ($P_{\text{value}} = 0.543$) and 15.13 ($P_{\text{value}} = 0.063$), respectively. F_{values} of both responses

were lower than F_{critical} ($F_{(0.05,3,2)} = 19.16$). Therefore, it can be used to confirm the precision of predicted equations.

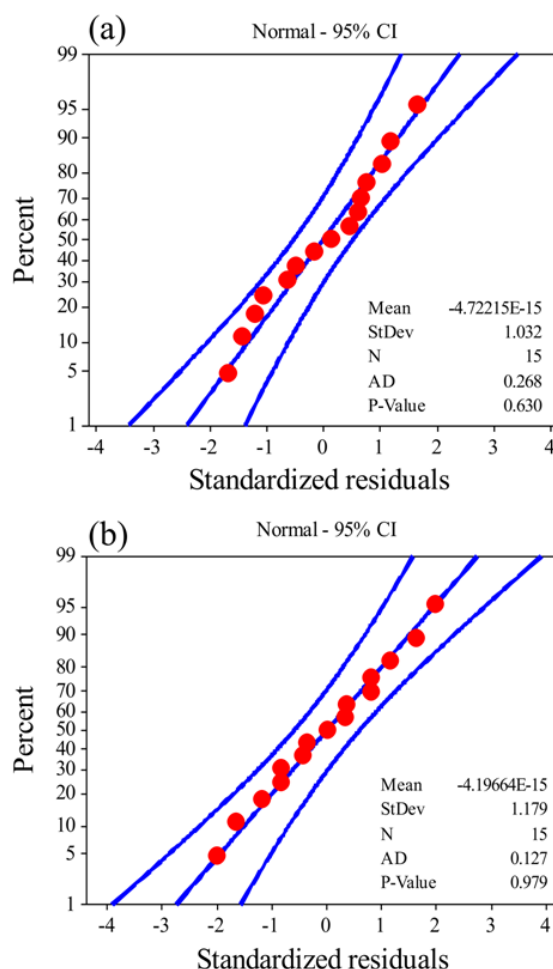


Figure 2 The probability plot of the standardized residual for (a) toluene removal and (b) $\text{Cu}^{3+}/\text{Cu}^{2+}$ mole ratio.

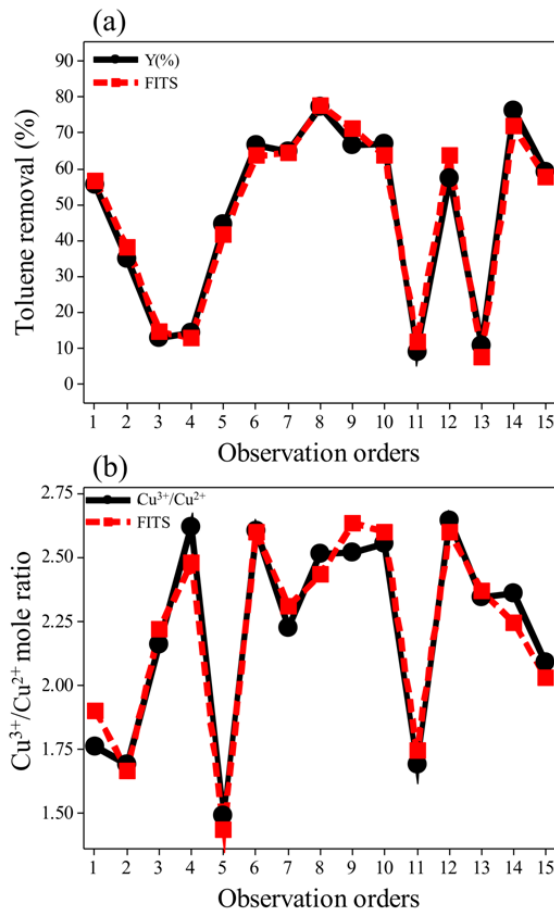


Figure 3 Time series plot of predicted value (FITS) and actual observed values of (a) toluene removal and (b) $\text{Cu}^{3+}/\text{Cu}^{2+}$ mole ratio.

2) Effect of Cu-K-OMS-2 synthesized conditions

Figure 4 shows the main and interaction effects of ageing temperature, ageing time and amount of Cu dopant on toluene degradation and $\text{Cu}^{3+}/\text{Cu}^{2+}$ mole ratio. Ageing temperature was found to have a significant effect on toluene removal (Figure 4(a)), corresponding to the P-value (<0.05) as shown in Table 3. Toluene removal efficiency increased when ageing temperature was increased from 55°C to 100°C. Thereafter, removal efficiency decreased slightly with an increase in ageing temperature from 100°C to 145°C. The results can be explained by the physical and chemical properties of Cu-K-OMS-2 material, such as the phase transformation of Cu-K-OMS-2 material and Cu^{3+} species on Cu-K-OMS-2 surface. Figure 5 shows the crystallinity of

catalysts, characterized by XRD, prepared at the same ageing time with various ageing temperatures and Cu content. The results indicated that at the lowest ageing temperature (55°C), the potassium-birnessite phase was only observed in amorphous phase. Then, the increasing of ageing temperature to 100°C and higher, cryptomelane phases were obvious in all samples. Thus, it can be concluded that the transformation of potassium-birnessite phase to the cryptomelane phase occurred when the ageing temperature was at 100°C [40-41], resulting in increased toluene removal. However, toluene removal decreased with an increase in the ageing temperature from 100°C to 145°C, which was explained by the presence of mixed-phase of CuO and bixbyite phase and the low crystallinity of cryptomelane, as shown in Figure 5. Additionally, the ageing temperature and amount of Cu dopant affected $\text{Cu}^{3+}/\text{Cu}^{2+}$ mole ratio (Figure 4(b)) which correlated with the tendency of toluene removal (Figure 4(a)). The high $\text{Cu}^{3+}/\text{Cu}^{2+}$ mole ratio influences on the enhancement of toluene removal. On the other hand, the ageing time showed an insignificant effect on both toluene degradation and $\text{Cu}^{3+}/\text{Cu}^{2+}$ mole ratio, corresponding to the P-value (>0.05) as shown in Table 3. According to the results, the slight decrease in toluene removal occurred with increased ageing time. Likewise, Millanar et al. [34] found that ageing temperature and ageing time of K-OMS-2 synthesis both influence toluene removal efficiency. Increasing the ageing time led to decreasing toluene removal. Toluene removal increased when ageing temperature was increased from 75°C to 120°C and then decreased above 120°C. In addition, increasing the amount of Cu dopant slightly increased toluene removal. Consequently, it can be concluded that ageing temperature and amount of Cu dopant exhibited a significant effect on toluene removal and $\text{Cu}^{3+}/\text{Cu}^{2+}$ mole ratio.

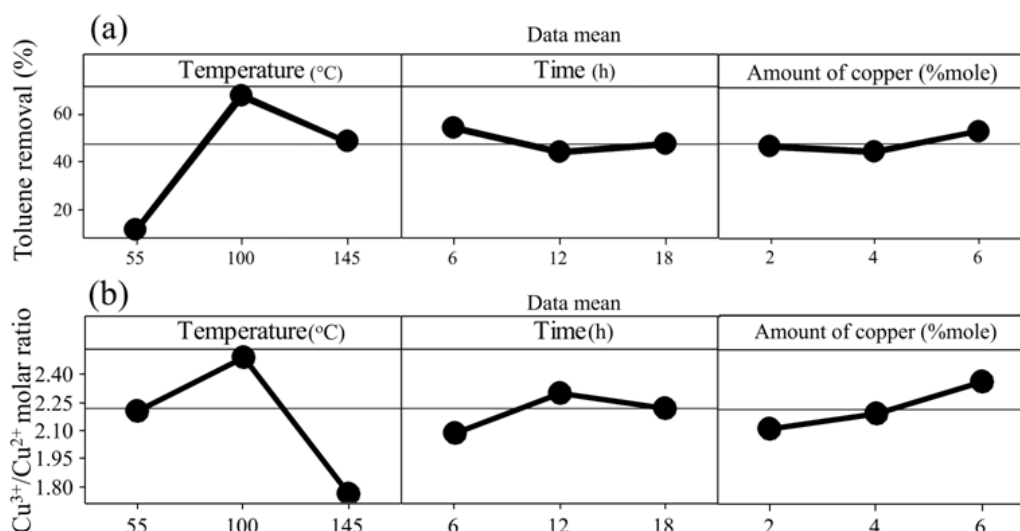


Figure 4 Main effects of ageing temperature, ageing time and amount of Cu dopant on (a) toluene degradation at 180°C of reaction temperature and (b) Cu³⁺/Cu²⁺ mole ratio.

3) Optimization results

The contour plot was used to confirm the interaction effects of independent variables and optimal condition ranges for Cu-K-OMS-2 synthesis using toluene removal as a response (Figure 6). Figure 6(a) shows the effect of ageing time and ageing temperature. The result showed that toluene removal was not affected by increasing ageing time or by increased ageing temperature from 55°C to 100°C. However, high toluene removal efficiency was obtained using an ageing time from 6-11 h and ageing temperature between 100-140°C. The effect of amount of Cu dopant together with ageing temperature is presented in Figure 6(b). The amount of Cu dopant showed an insignificant effect on toluene removal with increasing ageing temperature. However, a high amount of Cu dopant with the ageing temperature around 100-130°C exhibited high toluene removal efficiency. In addition, removal efficiency increased with higher levels of Cu dopant and lower ageing time (Figure 6(c)). Accordingly, the results clearly showed that the optimal conditions for Cu-K-OMS-2 synthesis are at high levels of Cu dopant (about 5-6% mole Cu-K-OMS-2), an ageing temperature

range from 100 - 130°C and a low ageing time (around 6-7 h).

The optimization processes include maximizing and/or minimizing of dependent and/or independent variables and responses. Primarily, for analyzing the effect of each variable on response, the appropriate model established following Eq. 2. Then, the goals were selected as maximizing toluene removal at 180°C of reaction temperature, in which the operating variables were in experimental ranges. Considering these goals, the maximum toluene removal (83.14%) obtains at 120°C of ageing temperature, 6h of ageing time and 6% mole of Cu on K-OMS-2 as shown in Figure 7.

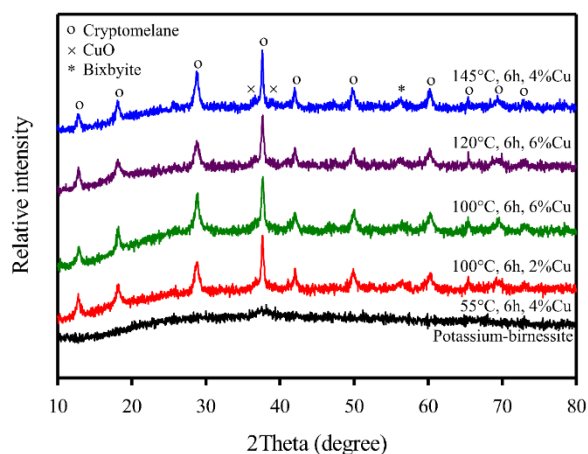


Figure 5 The XRD pattern of Cu-K-OMS-2 samples.

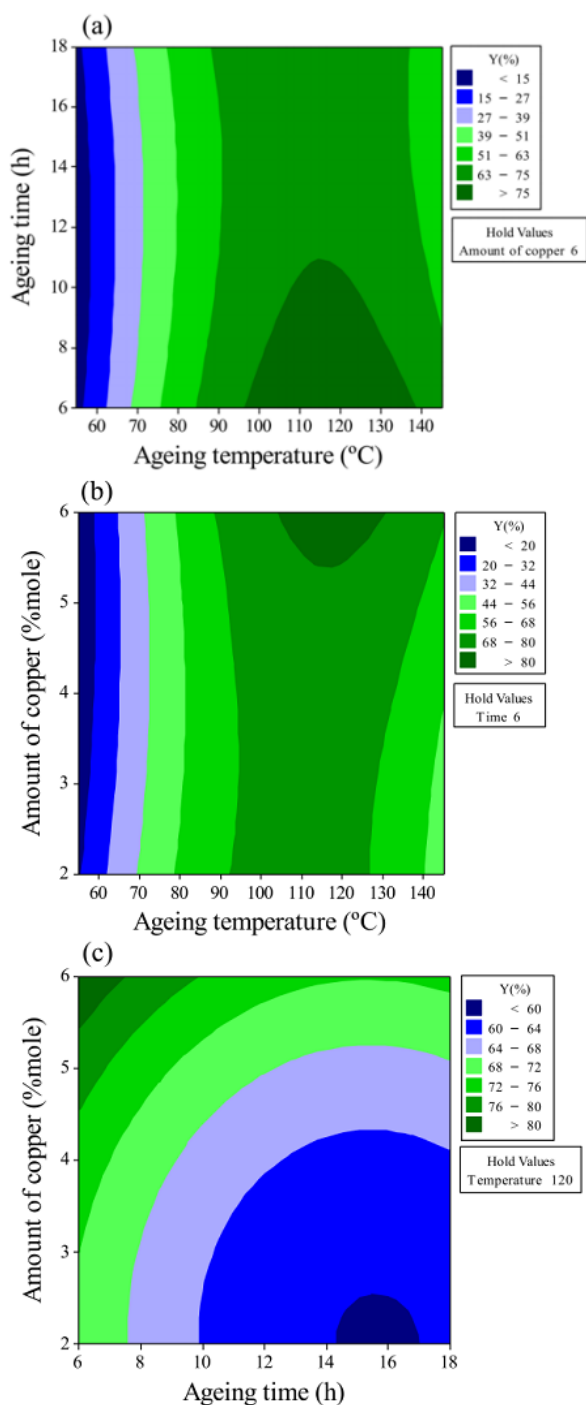


Figure 6 The contour plot of toluene removal at 180°C of reaction temperature. Figures showing the effect of (a) ageing temperatures along with ageing time, (b) ageing temperatures along with amount of Cu dopant and (c) ageing time along with amount of Cu dopant.

Consequently, the validation of the predicted equation was examined. We synthesized the best Cu-K-OMS-2 catalyst preparation under

optimal conditions. The Cu-K-OMS-2 catalyst was tested by reaction at 180°C with toluene oxidation. The percent removal results showed at about 80% of toluene removal. Hence, it can be concluded that the predicted equation can be used to compute the toluene removal. Moreover, the completed toluene oxidation occurred at 190°C of reaction temperature. Hence, Cu doped on K-OMS-2 catalyst can improve the catalytic activity at low temperature compared with the undoped K-OMS-2 catalyst [34].

Conclusions

Cu-K-OMS-2 catalysts can be synthesized by the *in situ* hydrothermal method. Ageing temperature and amount of Cu dopant showed a significant effect on both toluene removal and Cu³⁺/Cu²⁺ mole ratio. On the other hand, ageing time was insignificant for both responses. Increasing ageing temperature from 55°C to 100°C led to increasing Cu³⁺/Cu²⁺ mole ratio resulting to increased toluene removal. However, toluene removal decreased with increasing ageing temperature above 100°C due to the decrease in Cu³⁺/Cu²⁺ mole ratio. Additionally, the ageing temperature affected the transformation of potassium-birnessite phase to the cryptomelane phase, which also influences toluene removal. The optimal conditions for Cu-K-OMS-2 synthesis were found to be an ageing temperature of 120°C, ageing time of 6 hours and 6% mole of Cu dopant on K-OMS-2. These conditions resulted in 80% toluene removal at reaction temperature of 180°C.

Acknowledgements

The authors would like to acknowledge the financial support from the Research Center for Environmental and Hazardous Substance Management (EHSM), Khon Kaen University and the Graduate School, Khon Kaen University for supporting the admission of a

high potential student to study and research on his expert program in 2015 (Research No. 582T226). The authors would also like to express their gratitude to the Synchrotron Light Research Institute (Public Organization), Thailand for XPS measurement (SUT-SLRI: BL.5.3).

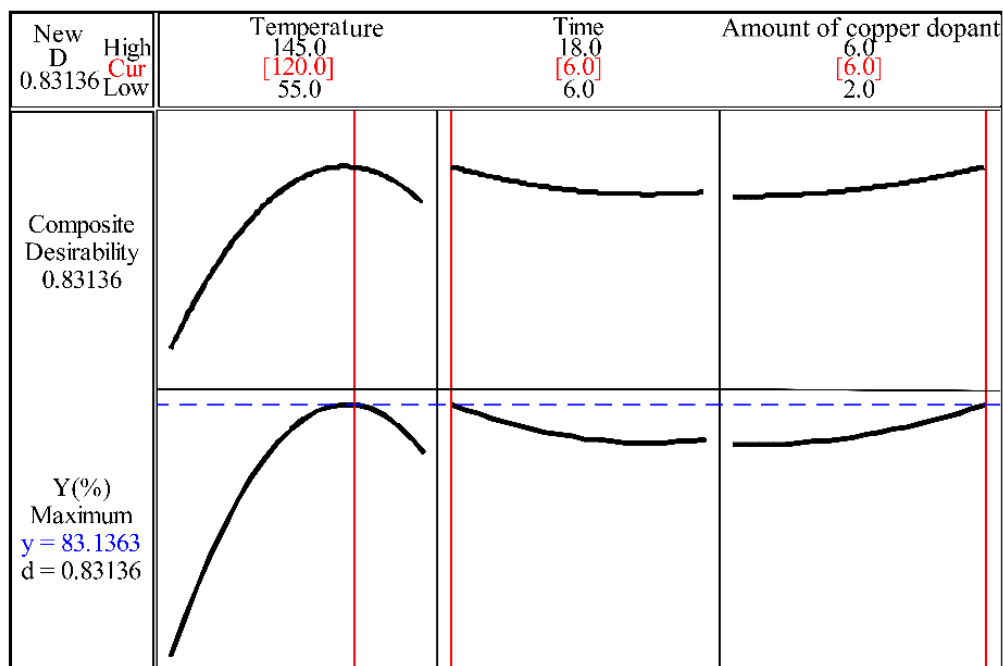


Figure 7 The optimization of hydrothermal conditions for Cu-K-OMS-2 synthesis on toluene removal.

References

- [1] Mandiracioglu, A., Akgur, S., Kocabiyik, N., Sener, U. Evaluation of neuropsychological symptoms and exposure to benzene, toluene and xylene among two different furniture worker groups in Izmir. *Toxicology and Industrial Health*, 2011, 27(9), 802-809.
- [2] Pariselli, F., Sacco, M.G., Ponti, J., Rembges, D. Effects of toluene and benzene air mixtures on human lung cells (A549). *Experimental and Toxicologic Pathology*, 2009, 61(4), 381-386.
- [3] Andrews L.S., Lee E.W., Witmer C.M., Kocsis, J.J., Snyder, R. Effects of toluene on the metabolism, disposition and hemopoietic toxicity of [3H]benzene. *Biochemical Pharmacology*, 1977, 26(4), 293-300.
- [4] Liu, F.F., Peng, C., Ng, J.C. BTEX in vitro exposure tool using human lung cells: Trips and gains. *Chemosphere*, 2015, 128, 321-326.
- [5] Edokpolo, B., Yu, Q.J., Connell, D. Health risk assessment of ambient air concentrations of benzene, toluene and xylene (BTX) in service station environments. *International Journal of Environmental Research and Public Health*, 2014, 11(6), 6354-6374.
- [6] Yoshikawa, M., Zhang, M., Toyota, K. Biodegradation of volatile organic compounds and their effects on biodegradability under co-existing conditions. *Microbes and Environments*, 2017, 32(3), 188-200.
- [7] Zhao, W., Cheng, J., Chen, Y., Wang, W. Degradation of selected indoor air pollutants: Comparison study of

- photocatalytic, ozone-assisted photocatalytic and amine adsorption processes. *Journal of Shanghai Jiaotong University (Science)*, 2012, 17(1), 13-19.
- [8] Rochetto, U.L., Tomaz, E. Degradation of volatile organic compounds in the gas phase by heterogeneous photocatalysis with titanium dioxide/ultraviolet light. *Journal of the Air & Waste Management Association*, 2015, 65(7), 810-817.
- [9] Zagoruiko, A.N., Mokrinskii, V.V., Veniaminov, S.A., Noskov, A.S. On the performance stability of the MnOx/Al₂O₃ catalyst for VOC incineration under forced adsorption-catalytic cycling conditions. *Journal of Environmental Chemical Engineering*, 2017, 5(6), 5850-5856.
- [10] Zhang J., Rao, C., Peng, H., Peng, C., Zhang, L., Xu, X., ..., Wang, X. Enhanced toluene combustion performance over Pt loaded hierarchical porous MOR zeolite. *Chemical Engineering Journal*, 2018, 334, 10-18.
- [11] Kamal, M.S., Razzak, S.A., Hossain, M.M. Catalytic oxidation of volatile organic compounds (VOCs) – A review. *Atmospheric Environment*, 2016, 140, 117-134.
- [12] Guisnet, M., Dégé, P., Magnoux, P. Catalytic oxidation of volatile organic compounds 1. Oxidation of xylene over a 0.2 wt% Pd/HFAU(17) catalyst. *Applied Catalysis B: Environmental*, 1999, 20(1), 1-13.
- [13] Balzer, R., Probst, L.F.D., Drago, V., Schreiner, W.H., Fajardo, H.V. Catalytic oxidation of volatile organic compounds (n-hexane, benzene, toluene, o-xylene) promoted by cobalt catalysts supported on γ -Al₂O₃-CeO₂. *Brazilian Journal of Chemical Engineering*, 2014, 31(3), 757-769.
- [14] Konova, P., Stoyanova, M., Naydenov, A., Christoskova, S.t., Mehandjiev, D. Catalytic oxidation of VOCs and CO by ozone over alumina supported cobalt oxide. *Applied Catalysis A: General*, 2006, 298, 109-114.
- [15] Genuino, H.C., Dharmarathna, S., Njagi, E.C., Mei, M.C., Suib, S.L. Gas-phase total oxidation of benzene, toluene, ethylbenzene, and xylenes using shape-selective manganese oxide and copper manganese oxide catalysts. *The Journal of Physical Chemistry C*, 2012, 116(22), 12066-12078.
- [16] Hernández, W.Y., Centeno, M.A., Romero-Sarria, F., Ivanova, S., Montes, M., Odriozola J.A. Modified cryptomelane-type manganese dioxide nanomaterials for preferential oxidation of CO in the presence of hydrogen. *Catalysis Today*, 2010, 1-4(157), 160-165.
- [17] Liu, J., Ke, L., Liu, J., Sun, L., Yuan, X., Li, Y., Xia, D. Enhanced catalytic ozonation towards oxalic acid degradation over novel copper doped manganese oxide octahedral molecular sieves nanorods. *Journal of Hazardous Materials*, 2019, 371, 42-52.
- [18] Luo, M., Cheng, Y., Peng, X., Pan, W. Copper modified manganese oxide with tunnel structure as efficient catalyst for low-temperature catalytic combustion of toluene. *Chemical Engineering Journal*, 2019, 369, 758-765.
- [19] Yun, L., Li, Y., Zhou, C., Lan, L., Zeng, M., Mao, M., ..., Zhao, X. The formation of CuO/OMS-2 nanocomposite leads to a significant improvement in catalytic performance for NO reduction by CO. *Applied Catalysis A: General*, 2017, 530, 1-11.
- [20] Hernández, W.Y., Centeno, M.A., Ivanova, S., Eloy, P., Gaigneaux, E.M., Odriozola, J.A. Cu-modified cryptomelane oxide as active catalyst for CO oxidation reactions. *Applied Catalysis B: Environmental*, 2012, 123-124, 27-35.

- [21] Sun, M., Yu, L., Ye, F., Diao, G., Yu, Q., Hao, Z., ..., Yuan, L. Transition metal doped cryptomelane-type manganese oxide for low-temperature catalytic combustion of dimethyl ether. *Chemical Engineering Journal*, 2013, 220, 320-327.
- [22] Tian, W., Liu, R., Wang, W., Yin, Z., Yi, X. Effect of operating conditions on hydrothermal liquefaction of *Spirulina* over Ni/TiO₂ catalyst. *Bioresource Technology*, 2018, 263, 569-575.
- [23] Song, Y.-Q., Liu, H.-M., He, D.-H. Effects of hydrothermal conditions of ZrO₂ on catalyst properties and catalytic performances of Ni/ZrO₂ in the partial oxidation of methane. *Energy & Fuels*, 2010, 24(5), 2817-2824.
- [24] Guo, X., Shen, J.-P., Sun, L., Song, C., Wang, X. Effects of hydrothermal treatment conditions on the catalytic activity of HZSM-5 zeolites in the methylation of 4-methylbiphenyl with methanol. *Catalysis Letters*, 2003, 87(3), 159-166.
- [25] Yoosuk, B., Song, C., Kim, J.H., Ngamcharussrivichai, C., Prasassarakich, P. Effects of preparation conditions in hydrothermal synthesis of highly active unsupported NiMo sulfide catalysts for simultaneous hydrodesulfurization of dibenzothiophene and 4,6-dimethyldibenzothiophene. *Catalysis Today*, 2010, 149(1), 52-61.
- [26] Mamaghani, A.H., Haghghat, F., Lee, C.-S. Photocatalytic oxidation of MEK over hierarchical TiO₂ catalysts: Effect of photocatalyst features and operating conditions. *Applied Catalysis B: Environmental*, 2019, 251, 1-16.
- [27] Suwannaruang, T., Rivera, K.K.P., Neramittagapong, A., Wantala, K. Effects of hydrothermal temperature and time on uncalcined TiO₂ synthesis for reactive red 120 photocatalytic degradation. *Surface and Coatings Technology*, 2015, 271, 192-200.
- [28] Bezerra, M.A., Santelli, R.E., Oliveira, E.P., Villar, L.S., Escalera, L.A. Response surface methodology (RSM) as a tool for optimization in analytical chemistry. *Talanta*, 2008, 76(5), 965-977.
- [29] Bashir, M.J.K., Aziz, H.A., Yusoff, M.S., Adlan, M.N. Application of response surface methodology (RSM) for optimization of ammoniacal nitrogen removal from semi-aerobic landfill leachate using ion exchange resin. *Desalination*, 2010, 254(1), 154-161.
- [30] Isgoren, M., Gengec, E., Veli, S. Evaluation of wet air oxidation variables for removal of organophosphorus pesticide malathion using Box-Behnken design. *Water Science and Technology: A Journal of the International Association on Water Pollution Research*, 2017, 75(3-4), 619-628.
- [31] Jung, K.-W., Kim, D.-H., Kim, H.-W., Shin, H.-S. Optimization of combined (acid+thermal) pretreatment for fermentative hydrogen production from *Laminaria japonica* using response surface methodology (RSM). *International Journal of Hydrogen Energy*, 2011, 36(16), 9626-9631.
- [32] Gengec, E., Ozdemir, U., Ozbay, B., Ozbay, I., Veli, S. Optimizing dye adsorption onto a waste-derived (modified charcoal ash) adsorbent using Box- Behnken and Central Composite design procedures. *Water, Air, & Soil Pollution*, 2013, 224(10), 1751.
- [33] Yodsa-nga, A., Millanar, J.M., Neramittagapong, A., Khemthong, P., Wantala, K. Effect of manganese oxidative species in as-synthesized K-OMS 2 on the oxidation of benzene. *Surface and Coatings Technology*, 2015, 271, 217-224.

- [34] Millanar, J.M., De Luna, M.D., Yodsana-Nga, A., Wantala, K. Toluene oxidation using K-OMS 2 synthesized via hydrothermal process by Central Composite design. *Chiang Mai Journal of Science*, 2018, 45(2), 1030-1038.
- [35] Doucet, N., Bocquillon, F., Zahraa, O., Bouchy, M. Kinetics of photocatalytic VOCs abatement in a standardized reactor, *Chemosphere*, 2006, 65(7), 1188-1196.
- [36] Rebhan, B., Tollabimazraehno, S., Hesser, G., Dragoi, V. Analytical methods used for low temperature Cu-Cu wafer bonding process evaluation. *Microsystem Technologies*, 2015, 21(5), 1003-1013.
- [37] Kataoka, T., Yamazaki, Y., Singh, V.R., Fujimori, A., Chang, F.-H., Lin, H.-J., ..., Wu, T. Ferromagnetic interaction between Cu ions in the bulk region of Cu-doped ZnO nanowires. *Physical Review B*, 2011, 84(15), 153203.
- [38] Natarajan, K., Saraf, M., Mobin, S.M. Visible light driven water splitting through an innovative Cu-treated- δ -MnO₂ nanostructure: probing enhanced activity and mechanistic insights. *Nanoscale*, 2018, 10(27), 13250-13260.
- [39] Liu, H., Wang, A., Sun, Q., Wang, T., Zeng, H. Cu nanoparticles/fluorine-doped tin oxide (FTO) nanocomposites for photocatalytic H₂ evolution under visible light irradiation. *Catalysts*, 2017, 7(12), 385.
- [40] Subramanian, N., Viswanathan, B., Varadarajan, T.K. A facile, morphology-controlled synthesis of potassium-containing manganese oxide nanostructures for electrochemical supercapacitor application. *RSC Advances*, 2014, 4(64), 33911-33922.
- [41] Birkner, N.R., Navrotsky, A. Thermodynamics of manganese oxides: Sodium, potassium, and calcium birnessite and cryptomelane. In *Proceedings of the National Academy of Sciences of the United States of America*, 2017, 114(7), 1451.